EUROPEAN ORGANIZATION FOR NUCLEAR RESEARCH
European Laboratory for Particle Physics

Large Hadron Collider Project

LHC Project Report 73

MODELLING BOUNDARY-INDUCED COUPLING CURRENTS IN RUTHERFORD-TYPE CABLES

A.P. Verweij

Abstract

In this paper it is shown that spatial distributions in the field-sweep rate and in the contact resistances along the length of Rutherford-type cables provoke a non-uniform current distribution during and after a field sweep. This process is described by means of Boundary-Induced Coupling Currents (BICCs) flowing through the strands over lengths far larger than the cable pitch. The dependence of the BICCs on the cable parameters (geometry, contact resistances etc.) is investigated by modelling the cable by means of a comprehensive network model. Working formulas are presented that give a first estimate of the characteristic time, the amplitude, and the characteristic length of the BICCs in any kind of magnet wound from a Rutherford-type cable. The results of these calculations show that BICCs can attain large values in multistrand cables, and hence play an important role in the ramp-rate limitation and field quality of high-field accelerator magnets even if the field-sweep rate is small.

LHC Division

ASC Pittsburgh '96

Administrative Secretariat
LHC Division
CERN
CH -1211 Geneva 23
Switzerland

Geneva, 15 November 1996

Modelling Boundary-Induced Coupling Currents in Rutherford-type Cables

A.P. Verweij
CERN, CHl211 Geneva 23, Switzerland

Abstract - **In this paper it is shown that spatial distributions in the field-sweep rate and in the contact resistances along the length of Rutherford-type cables provoke a non-uniform current distribution during and after a field sweep. This process is described by means of Boundary-Induced Coupling Currents (BICCs) flowing through the strands over lengths far larger than the cable pitch. The dependence of the BICCs on the cable parameters (geometry, contact resistances etc.) is investigated by modelling the cable by means of a comprehensive network model. Working formulas are presented that give a first estimate of the characteristic time, the amplitude, and the characteristic length of the BICCs in any kind of magnet wound from a Rutherford-$\dot{B}$type cable. The results of these caleulations show that BICCs can attain large values in multistrand cables, and hence play an important role in the ramp-rate limitation and field quality of high-field accelerator magnets even if the fieldsweep rate is small.**

I. INTRODUCTION

It is well known that Interstrand Coupling Currents (ISCCs) are generated in superconducting multistrand cables subject to a field variation $\dot{B}$. These ISCCs are usually calculated assuming that $\dot{B}$ and the contact resistances Ra (between adjacent strands) and Rc (between crossing strands) are uniform along the length of the cable. However, in all practical coils spatial variations of Ra, Rc and $\dot{B}$ are present along the length of the cable. For example, charging accelerator dipole and quadrupole magnets results in:

- Strong variations of $\dot{B}$, especially in the coil ends, for which $|\Delta \dot{B}/\Delta z|$ is of the same order as $|\dot{B}_{ce}/L_p|$, with $\Delta \dot{B}$ the change in $\dot{B}$ over the longitudinal length Δz, $\dot{B}_{ce}$ the field change in the aperture of the magnet and L_p the cable pitch.
- Weak variations, present in the entire coil, for which $|\Delta \dot{B}/\Delta z|$ is much smaller than $|\dot{B}_{ce}/L_p|$.

Note that in solenoid magnets mainly weak variations occur.

Besides spatial distributions of $\dot{B}$, spatial distributions of R_a and R_c are also present in an accelerator magnet and can be separated in:

- Variations over lengths far larger than L_p which are present in the entire cable since the transverse pressure varies considerably over the cross-section of the coil.
- Variations over lengths up to a few L_p which are especially present in the coil ends, in the soldered connections between different cables in the magnet and in local 'shorts' between strands.

The influence of spatial $\dot{B}$ and R_c-distributions on the coupling currents in Rutherford-type cables was also treated by Akhmetov et al., showing that the coupling currents vary periodically with a period equal to the cable pitch [1]. Also Krempasky and Schmidt have recently shown that non-

Manuscript received August 26, 1996.

uniform -distributions provoke additional coupling currents exhibiting very long time constants [2]. Their approach was based on the solution of the diffusion equation which they applied to a two-wire configuration coupled through a transverse conductance. Both approaches demonstrate *qualitatively* that non-uniformities in or the contact resistances always result in periodically varying coupling currents.

Quantitative results can be obtained using a comprehensive network model in which the cable is modelled by a network of nodes interconnected by strands and contact resistances [3,4]. In this paper the main results of these numerical calculations are evaluated by means of a new type of current, the so called *'Boundary-lnduced Coupling Current* (BICC)'. The term 'boundary' indicates that BICCs are generated by geometrical boundaries, boundaries in $\dot{B}$ and internal boundaries such as changes in R_a and mainly R_c. Variations in $\dot{B}$, R_a and R_c across the cable width only slightly change the distribution of the ISCCs but do not generate BICCs, and are therefore not dealt with in this paper.

The characteristic pattern of the BICCs and several analytical formulas for the magnitude and the characteristic time are given in sections III and IV, in the case of a step increase in $\dot{B}_\perp$ along the length of the cable. In section V it is explained how the formulas can be used to estimate the magnitude of the BICCs in a practical coil.

II. MODELLING BICCS

The network model, as extensively described in [4], is used to calculate the BICCs in a Rutherford-type cable (with width w, average height h and strand diameter d_s). Self- and mutual inductances between the strands are incorporated in the model. The longitudinal coordinate of the cable is denoted by z. The cable lengths from z=0 to the ends of the cable are referred to as $l_{cab,1}$, for z<0, and $l_{cab,2}$, for z>0. The end of the cable is either the physical end (with or without a cable-tocable connection) or a part where the strands are in the normal state (and hence have a relatively large strand resistivity). The strands are denoted by the *strand number i* (from 1 to the number of strands N_s).

The calculations are performed assuming that:

- The strands in the cable have the same length.
- The strand currents are smaller than the critical current.
- The BICCs 'see' an effective resistivity ρ_{bi} along the strand, which could be related to the diffusivity of the BICCs from the contacts into the filaments. Note that ρ_{bi} is not the same as the strand resistivity that the transport current 'sees' .

- R_a is much larger than R_c, and its influence on the BICCs is disregarded. See [4] for a treatment of $R_a << R_c$, which is e.g. the case for a cable with a resistive barrier between the two layers.
- Only the field change $\dot{B}_\perp$ perpendicular to the wide face of the cable is considered because the other field components turn out to have a much smaller effect.
- Only non-uniformities in $\dot{B}_\perp$ are dealt with since they are often the major cause of BICCs in coils. See [4] for a treatment of the influence of local R_c-variations (and uniform $\dot{B}$) which is important to estimate the BICCs due to R_c-variations in the coil ends and the cable-to-cable connections.
- The transport current is uniformly distributed among the strands.

In the following the term 'steady-state' denotes the condition that the cable is exposed to a certain $\dot{B}_\perp$ distribution for a time much larger than all characteristic times involved.

Most of the simulations are performed by subsequently changing all the parameters in the network model, namely h, w, L_p, N_s, R_c, R_a, ~ $\dot{B}_\perp$ and ρ_{bi}. The results are presented as analytical formulas that describe the dependence of the currents, time constants and decay lengths on the above-mentioned parameters. Hence, each analytical relation contains one or more constants of proportionality that are needed to fit the numerical results to the analytical expressions.

III. CHARACTERISTIC BICC PATTERN

The characteristic BICC pattern is illustrated for a 16-strand cable exposed to a field change $\dot{B}_\perp$ of 0 for $z<0$ and 0.01 Ts^{-1} for $z\geq 0$ (with $R_c=1\ \mu\Omega$, $R_a= 10\ \mu\Omega$, $d_s= 1.3$ mm and $L_p=100$ mm). In Fig. 1a/b the current I_{str} in two strands is depicted, showing that the strand current can be regarded as a superposition of three components:

- The transport current which is constant all along the strand (and equal to 20 A in this case).
- The oscillating term, with an average equal to 0, related to the ISCCs which are mainly present for $z\geq 0$. The amplitude of the ISCC pattern is about 7 A and remains constant for $z\geq 0$.
- The BICC which is maximum close to the $\dot{B}_\perp$-step and decays along the cable length.

Two regimes can be distinguished for the BICCs:

Regime A. The BICCs decay quasi-exponentially along the length and approach 0 clearly before the end of the cable. In this case a characteristic length ξ of the BICCs can be defined as the length over which the BICCs decay to l/e of their maximum value.

Regime B. The BICCs decay quasi-linearly towards 0 at the end of the cable.

The ratio between R_c and ρ_{bi} is the main factor that determines the regime of the BICCs (see section IV).

A regular pattern exists in the magnitudes of the BICCs. In each cross-section of the cable opposite strands carry BICCs with the same magnitude but with an opposite sign. Adjacent strands have only slightly different BICCs.

The regular pattern is typical for BICCs and causes them to generate more pronounced field errors in magnets than in the case of a random current distribution among the strands, such as that caused by different joint resistances.

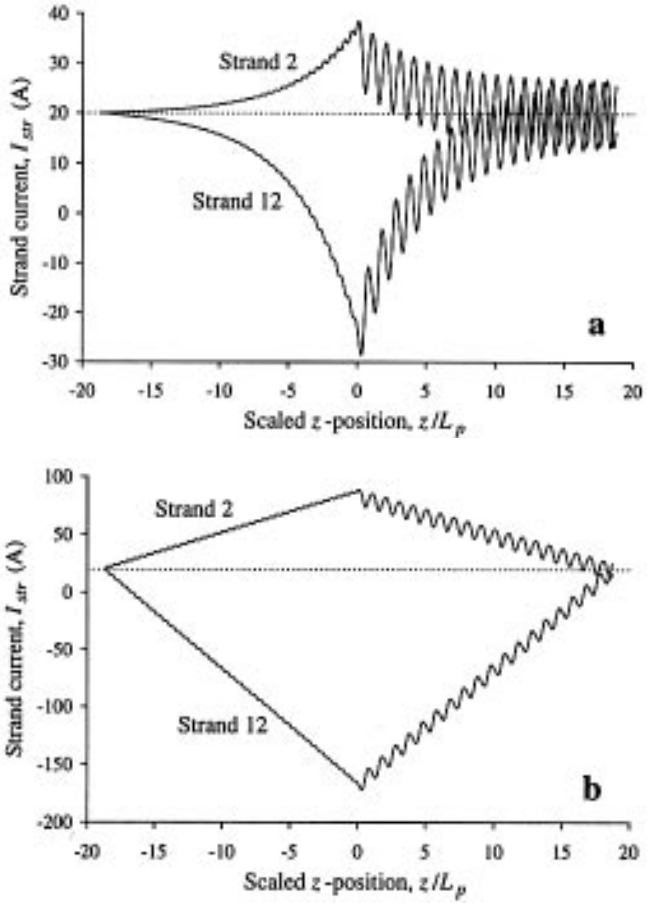

Fig. l. The characteristic pattern of the currents in two strands of a Rutherford-type cable subject to field changes of 0 for $z<0$ and 0.01 Ts^{-1} for $z\geq 0$. The transport current is shown by a dotted line. **a**: Regime A: ρ_{bi} =2 10^{-14} Ωm, **b**: Regime B: ρ_{bi} =2 10^{-17} Ωm.

The change of the BICCs in axial direction corresponds to the cross-over currents l_c flowing between the upper and lower layers through R_c. This in turn results in a periodic behaviour of l_c and, therefore, the coupling power $P_c\left(=I_c^2 R_c\right)$ along the cable length. So, parts having large and small local power losses alternate, which is shown in Fig. 2 where the coupling power loss in each resistance R_c *is* depicted over a length of *3* L_p.

Half of the strands are less heated than the average since they 'slalom' in between the hot spots. These strands correspond to those with small BICCs. The other half of the strands, which carry large BICCs, are heated more than the average. Hence, the spots with a large local power loss correspond to those areas where strands with large BICCs cross each other. During ramping, the stability of a coil is therefore affected since some strands have significant larger current than the transport current and are heated more than the average. However, if the thermal conductivity inside the cable

is good the temperature of the strands will probably be quite uniform even if the power loss fluctuates strongly.

Note that, due to the large characteristic lengths, the BICCs can cause a significant enhancement of the coupling

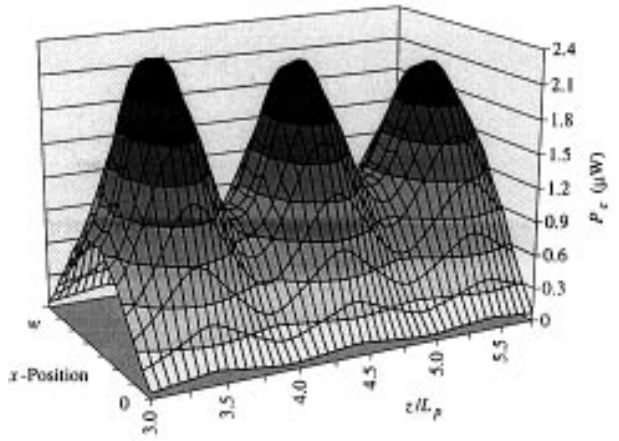

Fig. 2. The characteristic pattern of P_c across the cable width (with w= 10.4 mm) and along the length of a Rutherford-type cable subject to field changes of 0 for z<0 and 0.01 Ts^{-1} for z≥0 (Regime A: ρ_{bi} = 2 10^{-14} Ωm).

power loss, also in those parts of the cable which are not exposed to the local $\dot{B}_\perp$.

It is important that the the decay of the BICCs along the length is only quasi-exponential or quasi-linear if R_c *is* constant. In the case of a cable with a longitudinal R_c variation, the change of the BICCs along the cable length will vary according to the local R_c. This implies that, for example, the slope dI_{bi}/dz of the linear decay shown in Fig. 1b will not be constant along the length but wil1 locally increase (decrease) in sections with smaller (larger) R_c. This means that all the sections in a cable having a small R_c could enhance the magnitude of the BICCs, even if these sections are placed in a low-field region of the magnet. A typical example is the joint between the cables of two poles. Experimental evidence of the influence of a local decrease in R_c on the magnitude of the BICCs is given in [5].

IV. QUANTITATIVE RESULTS

The BICCs are characterised by an amplitude, a propagation length and a characteristic time. The development of the BICCs in time is a complicated process which shows a certain similarity with electromagnetic waves having a propagation velocity, and attenuation and dispersion along the length. In this paper the transient behaviour of the BICCs is summarised by means of the average characteristic time $\tau_{bi,av}$, i.e. the time during which the average of the absolute value of all the BICCs in the whole cable decays to 1/e of its initial value.

Note that the BICCs can only attain the steady-state values if the total current in each strand section remains smaller than the critical current, and if the characteristic time of the BICCs is smaller than the time during which the cable is exposed to a field change.

The following analytical relations for regimes A and B are derived by a fit to the numerical calculations using the network model in the case of a straight cable having strands with a round cross-section. The errors in the fitting constants are about 5-10% (for $8 \le N_s \le 40$).

Regime A.

The steady-state BICC $I_{bi,i}$ in strand i can be approximated by (neglecting the small periodic signal for z<0):

$$I_{bi,i}(z) = I_{bi,0}\sin(2\pi(i-0.5)/N_s)e^{-|z|/\xi} \quad [\mathrm{A}], \qquad (1)$$

$$\text{with:} \quad I_{bi,0} = 0.88\frac{w\xi}{R_c}\left(1-e^{-N_s/9.6}\right)\Delta\dot{B}_\perp \quad [\mathrm{A}], \qquad (2)$$

$$\text{and:} \quad \xi = 0.50\sqrt{\frac{R_c L_p \pi d_s^2}{2\rho_{bi}N_s}} \quad [\mathrm{m}]. \qquad (3)$$

ξ can be large for practical superconductors especially for small ρ_{bi} and large R_c The characteristic time $\tau_{bi,av}$ satisfies:

$$\tau_{bi,av} = 1.2\cdot 10^{-8}\frac{N_s \pi d_s^2}{\rho_{bi}} \quad [\mathrm{s}], \qquad (4)$$

where the constant has the dimensions $\Omega\mathrm{sm}^{-1}$. Note that $\tau_{bi,av}$ is independent of R_c.

Regime B.

A similar expression for $I_{bi,i}$ is obtained as eq. l with the difference that the BICCs depend linearly on the cable length:

$$I_{bi,i}(z) = I_{bi,0}\sin\left(2\pi(i-0.5)/N_s\right)\left(1-|z|/l_{cab,i}\right) \quad [\mathrm{A}], \qquad (5)$$

$$\text{with:} \quad l_{cab,i}=l_{cab,1} \text{ for } z<0 \text{ and } l_{cab,i}=l_{cab,2} \text{ for } z\ge 0,$$

$$\text{and:} \quad I_{bi,0} = 1.0\frac{w l_{cab,eff}}{R_c}\left(1-e^{-N_s/9.6}\right)\Delta\dot{B}_\perp \quad [\mathrm{A}], \qquad (6)$$

$$\text{and:} \quad l_{cab,eff} = 2\frac{l_{cab,1}l_{cab,2}}{l_{cab,1}+l_{cab,2}} \quad [\mathrm{m}]. \qquad (7)$$

The time constant $\tau_{bi,av}$ is now related to the lengths $l_{cab,1}$ and $l_{cab,2}$ and can be expressed by:

$$\tau_{bi,av} = 6.2\cdot 10^{-8}\frac{l_{cab,1}l_{cab,2}N_s^2}{L_p R_c} \quad [\mathrm{s}], \qquad (8)$$

where the constant has the dimension $\Omega\mathrm{sm}^{-1}$. Note that for $l_{cab,1}= l_{cab,2} = l_{cab}/2$ the characteristic time $\tau_{bi,av}$ is about a factor (l_{cab}/L_p) larger than the average time constant of the ISCCs, i.e. ca. $1.6.10^{-8}\ L_p N_s^2/R_C$ [4].

The maximum magnitude $I_{bi,0}$ of the BICCs for practical cables (i.e. N_s *is* about 20-40) *is,* in first approximation, about a factor ξ/L_p (regime A) or $l_{cab,eff}/L_p$ (regime B) larger than the maximum ISCC, i.e. ca. $0.042 L_p w N_s \dot{B}_\perp/R_c$ [5]. This factor explains the large magnitude of the BICCs shown in Fig. 1a/b where $\xi \approx 4L_p$ and $L_{cab,eff} \approx 18 L_p$ for the given simulation parameters.

V. ESTIMATING BICCS IN COILS

The magnitude of the BICCs due to any distribution of $\dot{B}_\perp$ along the cable length, simulating e.g. the coil ends or the part where the cable enters the coil, can be modelled

directly with the network model. It is also possible to replace (1) by a multi-step function:

$$I_{bi,I}(z) = \sum_{m=0}^{N_s-1} I_{bi,0,m} \sin\left(\frac{2\pi(i-0.5+m)}{N_s}\right) e^{-|z-mL_p/N_s|/\xi} \quad [\mathrm{A}], \quad (9)$$

with:

$$I_{bi,0,m} = 0.88\frac{w\xi}{R_c}\left(1-e^{-N_s/9.6}\right)\Delta\dot{B}_{\perp,m} \quad [\mathrm{A}]. \quad (10)$$

and $N_B=l_{cab}N_s/L_p$, *and* $z=mL_p/N_s$. This approach is valid as long as the set of equations is completely linear, i.e. as long as the strands are not saturated and ρ_{bi} is independent of the current through the strand. A similar summation can of course be made for regime B by combining (5)-(7).

It can be easily seen that the BICCs are maximum if the $\dot{B}_\perp$-transition happens in a single step, since the summation in (9) can never be larger than $I_{bi,0}$ as defined by (2). In general it can be said that strong variations (i.e. $|\Delta \dot{B}_\perp/\Delta z|$ of the same order as $|\dot{B}_{\perp,max}/L_p|$), cause large BICCs whereas weak variations, i.e. $|\Delta \dot{B}_\perp/\Delta z| << |\dot{B}_{\perp,max}/L_p|$, cause small BICCs.

In a practical coil, due to the numerous R_c- and $\dot{B}_\perp$-variations located at different positions, there is of course a large quantity of BICCs each having their own magnitude and characteristic time and length. Usually, it is therefore only possible to speak about average values for $I_{bi,0}$, ξ and τ_{bi}.

Note that $\tau_{bi,av}$ in a coil can change (compared to a straight cable) due to the mutual inductances between the BICCs of the various turns, and can be a few times smaller or larger than $\tau_{bi,av}$ in a single straight cable.

An estimate of the BICCs of regime A still requires a proper value of ρ_{bi}, in order to calculate ξ and $\tau_{bi,av}$. Probably the most convenient way is to measure either ξ or $\tau_{bi,av}$. in a coil and deduce ρ_{bi} from it. $\tau_{bi,av}$ can be measured by measuring the characteristic time of the sinusoidally varying field errors in the coil that are proportional to the field sweep rate $\dot{B}$. ξ *is* more difficult to measure but can (especially in long accelerator magnets) sometimes be deduced from the decay of the sinusoidally varying field errors (that are proportional to $\dot{B}$) along the length. In the LHC dipole model magnets ξ is typically a few meters, τ_{bi}. between l00 and l000 s and ρ_{bi} about 10^{-14} Ωm [4],[6].

Note that even at small field-sweep rates the BICCs can become relatively large. For example, $I_{bi,0}$=50 A for N_s=*28,* w=0.015 m, ξ=4m, R_c=10μΩ and $\Delta \dot{B}_\perp$=0.0l Ts^{-1} (regime A).

If ξ is calculated to be larger than the length between the cable non-uniformity and the ends of the cable, then the BICCs have to be calculated using the formulas for regime B. If ξ is of the same order as $l_{cab,1}$ (or $l_{cab,2}$) then the exact BICC pattern cannot be described by simple analytical relations but the relations for regime A or B can be used as a first approximation.

V. CONCLUSION

So-called Boundary-Induced Coupling Currents (BICCs) are generated in (Rutherford-type) cables, which are exposed to a varying field, if the field sweep rate or the contact resistances vary along the cable length.

BICCs differ from the 'normal' Interstrand Coupling Currents because they stay in the strands over long distances of 10-10^3 times the cable pitch (or the length of the cable). BICCs propagate through the cable and exhibit large characteristic times of 10-10^5 s (for practical cables) which are several orders of magnitude larger than the time constant of the Interstrand Coupling Currents.

In accelerator magnets the BICCs cause:

- sinusoidally varying field distortions along the magnet axis with a large characteristic time, an amplitude proportional to the field sweep rate and a period equal to the cable pitch,
- an increase in the coupling power,
- a decrease of the stability of the cable since some strands carry more current than the transport current and since these strands are heated more than the average.

The decay of the BICCs along the length of the cable is either quasi-exponential (regime A) or quasi-linear (regime B), which is determined by the ratio between R_c and the effective strand resistivity that the BICCs "see". The slope of the decay varies according to the local R_c in the cable.

The BICCs are mainly caused by variations in the field change $\dot{B}_\perp$ transverse to the cable width, and their magnitude increases strongly if the lengths of the $\dot{B}_\perp$ variations are of the same order or smaller than the cable pitch. In the case of a dipole magnet this implies that the field variations in the coil ends cause large BICCs whereas the gradual variation of $\dot{B}_\perp$ to which the total cable is exposed only causes relatively small BICCs.

The magnitude of the BICCs can be reduced by increasing the contact resistances R_a and especially R_c. However, local decreases in R_c (e.g. in the cable-to-cable connections) could significantly increase the magnitude and the characteristic time of the BICCs. This implies that also in cables having a large R_c, BICCs will be present if the cable is locally soldered (even if the soldered parts are located in a low-field region).

REFERENCES

[l] A.A. Akhmetov, A. Devred, and T. Ogitsu, "Periodicity of crossover currents in a Rutherford-type cable subjected to a time-dependent magnetic field", J *Appl. Phys., vol.* 75 (6), pp. 3176-3183, 1994.

[2] Krempasky, C. Schmidt, "Influence of a longitudinal variation of dB/dt on the magnetic field distribution of accelerator magnets", *Appl. Phys. Lett., vol* . 66(12), pp. 1545- 1547, 1995.

[3] A.P. Verweij, and H.H.J. ten Kate, "Super Coupling Currents in Rutherford type of cables due to longitudinal non-homogeneities of dB/dt", *IEEE Trans. On Appl. SC, vol.* 4, p. 404-407, 1995.

[4] A.P. Verweij, *Eiectrodynamics of Superconductlng Cables in Accelerator Magnets*, PhD thesis University of Twente, The Netherlands, 1995.

[5] A.P. Verweij, M.P. Oomen, and H .H .J. ten Kate, "Boundary-lnduced Coupling Currents in a 1.3 m Rutherford-type cable due to a locally applied field change", unpublished (paper LDA-5 at ASC'96, Pittsburgh, USA).

[6] L. Bottura, Z. Ang, and L. Walckiers, "Expeimental evidence of Boundary-lnduced Coupling Currents in LHC prototypes", unpublished (paper LQB-4 at ASC'96, Pittsburgh, USA).